Published in final edited form as:
RSC Adv. 2013 November 21; 3(43): 21054–21061. doi:10.1039/C3RA42394H.

Ionic Liquid-Based Fluorescein Colorimetric pH Nanosensors

Susmita Das[*], **Paul K. S. Magut**, **Sergio L. de Rooy**, **Farhana Hasan**, and **Isiah M. Warner**[*]
Department of Chemistry, Louisiana State University, Baton Rouge, LA-70803, USA.

Abstract

A novel pH sensitive, colorimetric ionic liquid nanosensor based on phosphonium salts of fluorescein is reported. Herein, fluorescein salts of various stoichiometries were synthesized by use of a trihexyltetradecylphosphonium cation $[TTP]^+$ in combination with dianionic $[FL]^{2-}$ and monoanionic $[FL]^-$ fluorescein. Nanomaterials derived from these two compounds yielded contrasting colorimetric responses in neutral and acidic environments. Variations in fluorescence spectra as a function of pH were also observed. Examination of TEM and DLS data revealed significant expansion in the diameter of $[TTP]_2[FL]$ nanodroplets in acidic environments of variable pHs. A similar trend was also observed for [TTP][FL] nanoparticles. The pH dependent colorimetric and other optical properties of these nanomaterials are attributed to alterations in molecular orientations and stacking as suggested by measuring the absorption, fluorescence, and zeta potential. Since the pH is an important indicator for many diseases, including cancer, these nanosensors are considered to be potential candidates for biomedical applications.

Keywords

room temperature ionic liquids; colorimetric; fluorescein; phosphonium; pH; J-aggregates

Introduction

Smart materials capable of application as inexpensive sensing tools using a simple colorimetric approach are highly desirable for analysis and diagnosis. One of the most important rationales for this observation is colorimetric detection techniques minimize the need for more sophisticated instrumentation. Numerous nanoparticles have been developed for colorimetric biosensing, including gold, silver, graphene oxide, and carbon nanotubes.[1] Color changes observed due to aggregation and disaggregation of these nanoparticles have also been used as methods for detection of several biomaterials.[1] For example, magnetic nanoparticles such as Fe_3O_4 undergo color change due to the catalysis of peroxidase subtrates.[2,3] Aptamer-based colorimetric sensors are also reported, where aptamer binding events are transformed into a colorimetric response.[4] Colorimetric detection of adenosine and cocaine has also been performed using such sensors.[4]

[*]Corresponding authors, susmita@lsu.edu and iwarner@lsu.edu, Fax: 225-578 3971; Tel: 225-5782829.

Supporting Information Available: Synthesis of ILs and characterization (FTIR, NMR, TGA), Synthesis of nanosensors, zeta potentials.

The pH balance in mammalian tissues can be altered under several health conditions such as cancer, chronic pulmonary diseases, and renal failure.[5] The extracellular pH value usually lies in the range of 5 – 7 under various pathological conditions. Certain bacterial infections also produce an acidic environment where the pH may vary between 4.5 – 7.0.[6] On the basis of this observation, pH sensitive polymeric nanoparticles as well as nanoparticles embedded in pH sensitive gel matrices have been designed for local delivery of antibiotics.[6] Tumors and cancerous tissues have been found to exhibit acidic pH values as compared to normal tissues due to the production of lactic acid as well as hydrolysis of ATP in the hypoxic regions of tumors.[5] Thus, several pH responsive nanoparticles have been applied to stimuli responsive drug delivery for tumors and cancerous sites,[7] through exploitation of their acidic environment.

As pH is an important indicator for advancement of numerous diseases and biological processes, development of smart nanomaterials for simple detection of pH using a colorimetric approach, in combination with additional measurable pH dependent parameters, is highly desirable. In this regard, various metal nanoparticles based colorimetric pH sensors have been reported, including modification of gold or silver nanoparticles with DNA,[8] protein antigens,[9] and polymers.[10] Although several nanomaterials have been designed toward this end, most of these materials involve multistep and very sophisticated synthetic procedures. Thus, a facile, cost efficient design in this direction would be extremely advantageous.

Room temperature ionic liquids (RTILs) have been applied to multiple analytical techniques such as separation science, MALDI-MS, quartz crystal microbalance sensors, as well as in synthetic chemistry as catalysts and solvents in electroanalysis.[11] Due to their versatility, several ionic liquids have been prepared using various combinations of ions in order to obtain desired properties. For example, a recent communication reports an RTIL-based colorimetric amine sensing on films.[12] In another study, ILs have been synthesized using indicator dyes and their pH sensitive properties have been investigated.[13] A recent report describes the design of an ionic liquid polymer gel-based barcode system derived from indicator dyes for determining the pH of sweat generated during an exercise period.[14] However, to the best of our knowledge, nanosensors based on RTILs with pH dependent colorimetric and morphological response have not yet been reported. Optical nanosensors for a variety of sensing applications including pH have been developed by Kopelman and co-workers which involve encapsulation of dyes in polymeric nanoparticles.[15] However, pH dependent colorimetric and size changes have not been observed in such studies. Moreover, problems such as leaching and alteration of photophysical properties are often encountered upon encapsulation of fluorphores.[15] In recent years, our group has introduced nanoparticles derived from a ***g***roup of ***u***niform ***m***aterials ***b***ased on ***o***rganic ***s***alts (GUMBOS), which are higher melting (solid phase) counterparts of ionic liquids with much wider scopes of variations. We have reported functional, as well as multifunctional nanoGUMBOS with various morphologies and spectral features.[16, 17, 18]

Herein, we report the synthesis, characterization, and pH dependent properties of two novel nanomaterials based on RTILs derived from FL and TTP ions of two different stoichiometries. The present study involves development of nanosensors directly from a

fluorophore in contrast to studies reported in the literature where the fluorophore is either encapsulated or covalently linked to polymeric nanoparticles.[15, 19] The pH dependent optical and morphological properties of these nanosensors suggest their potential utility for applications in detection, *in vitro* pathological applications, as components for pH and size dependent chemical separation,[20] as well as pH sensitive drug delivery devices.[21]

Results and Discussions

Aqueous solutions of disodium fluorescein (Na_2FL has been known to exhibit pH sensitive spectral changes which are attributable to the presence of different ionic forms of fluorescein.[22] However, to the best of our knowledge and as demonstrated in this study, Na_2Fl is not known to exhibit any significant pH dependent colorimetric response. Moreover, Na_2FL is highly soluble in aqueous medium and thus nanoformulation is not possible.

Herein, hydrophobic salts of fluorescein were synthesized in two different stoichiometries in combination with TTP counterions. The bulky TTP cation not only induces hydrophobicity in the resulting salt but also drops its melting point below or close to room temperature resulting into the formation of fluorescein based ILs. Hydrophobic properties were introduced in order to obtain fluorescein nanoparticles with pH sensitive spectral properties. The initial idea was to achieve these properties when these nanoparticles were suspended in aqueous medium for expansion of their applications as stimuli responsive carriers for therapeutic agents. However, the synthesized nanodroplets unexpectedly exhibited numerous pH sensitive effects, as well as potential therapeutic characteristics which may allow enormous applications of these new materials.

Physical Characterization of the ILs

Two ILs were synthesized using ion metathesis reactions in two different stoichiometric ratios yielding the salts $[TTP]_2[FL]$ and [TTP][FL]. $[TTP]_2[FL]$ was an orange viscous liquid at room temperature, while the latter, [TTP][FL], was a dark orange sticky solid (Figure S1). A variation in their viscoelastic properties was expected, since the presence of two bulky cations leads to further frustrated packing,[23] resulting in a lower melting IL. Thermogravimetric analyses of these compounds suggested a fairly high decomposition temperature for both compounds. $[TTP]_2[FL]$ was stable up to 348.6 °C, while [TTP][FL] exhibited a decomposition temperature of 354.6 °C.

Optical Properties of pH Dependent TTP Nanomaterials

Nanomaterials derived from the two fluorescein-based ILs through a reprecipitation[18] technique produced contrasting pH dependent colorimetric responses. The $[TTP]_2[FL]$ nanodroplet suspension exhibited a red color in water whose inherent pH was 8.4 and in phosphate buffer of pH 7.4. These nanodroplets displayed distinct color changes with further variations of buffer pH (universal buffer)[24] in the acidic region. In a buffer of pH 5.5, the solution was orange, orange green at pH 4, and light green at pH 2.2 (Figure 1a). However, [TTP][FL] nanoparticles did not exhibit a significant color change as a function of changes in pH value (Figure 1b). A control experiment was also performed with the parent

compound (Na_2FL) at the same concentration, which displayed little or no pH dependent colorimetric response (Figure 1c).

Absorption spectra of $[TTP]_2[FL]$ nanodroplets revealed a 23 nm red-shift in unbuffered water and a 40 nm red-shift in buffer of pH 7.4, as compared to the same concentration of the parent compound (Na_2FL) in the corresponding media. A red shift in the absorption spectrum of a dye is usually attributed to head to tail type of stacking, often referred to as J-type aggregation.[18]

A gradual blue shift in absorption maxima was observed with a lowering of the pH value below 7.4 (Figure 2a). In spite of this blue shift in acidic buffers, the absorption maxima of the nanomaterials were red-shifted as compared to the parent compound. This observation suggests J-type aggregates of various stacking angles in different pH environments, which results in variable red-shifts.[25] In order to further confirm this as an aggregation effect and not just the inherent characteristic of this IL, concentration dependent absorption spectra were collected. Examination of these spectra indicated that the absorption maxima were identical with those of the parent compound (490 nm) in the micromolar region. A concentration dependent change in shape and position of the absorption spectra and a complete red-shift in the absorption peak at higher concentrations further confirmed this as an aggregation effect and thus the red shift is attributed to J-type of aggregation within these nanomaterials at higher concentrations.[18]

In addition to the observed colorimetric response, $[TTP]_2[FL]$ nanodroplets were also observed to display a pH dependent fluorescence emission and excitation spectra. In water (pH 8.4) and pH 7.4 buffer, the fluorescence emission and excitation spectra of the $[TTP]_2[FL]$ nanodroplets (50 μM) were red-shifted as compared to the parent compound (Na_2FL) and to the same compound ($[TTP]_2[FL]$) at lower concentrations. In an acidic environment, the fluorescence spectrum was gradually blue-shifted towards the monomeric region, also suggesting a change in molecular stacking with pH (Figure 2).[18, 25] It is worth noting that the stokes shift of these nanomaterials was extremely low and, in some cases (at pH 7.4 and 5.4), nearly resonance fluorescence was observed, which is a well established signature of J-aggregation.[18] In addition to the red-shifted absorption spectra and the small stokes shifts (Figure 2), J-aggregation was also confirmed by use of fluorescence lifetime measurements. Lifetime studies suggested that in water and at pH 7.4, $[TTP]_2[FL]$ nanodroplets were found to be composed entirely of a shorter lifetime component (73 ps) which is characteristic of J-aggregates as compared to its lifetime of 4 ns in the monomeric state in water. The monomeric lifetime was found to be similar to that of the parent compound in an aqueous medium.[26] The relatively lower fluorescence intensity of $[TTP]_2[FL]$ J-aggregates is attributed to the formation of higher order aggregates which leads to quenching.[27]

Although, [TTP][FL] nanodroplets did not demonstrate any significant pH dependent color change, shifts (Fig 3d) and the appearance of distinct peaks/shoulders in the absorption spectra with varying pH suggest a similar change in molecular aggregation for various pH environments.[18] The fluorescence emission maxima in water was centered around the monomeric emission region (513 nm), revealing that the predominant emitting species were

likely monomers, which is also complemented by a two component fluorescence lifetime decay with 79% contribution from the monomer with a lifetime of 3.9 ns and 21% contribution from a 109 ps component attributed to J-aggregates. The fluorescence emission maxima of [TTP][FL] at all pH values being centred on 513 nm is consistent with the fact that the primary fluorescence emission was contributed by the monomeric component. The decrease in fluorescence emission was however attributed to the formation of weakly fluorescent or non-fluorescent aggregates in various pH environments.

Thus, it can be summarized from the optical properties that the presence of two TTP cations favors J-aggregation to a greater extent as compared to one TTP cation. The two bulky TTP cations probably force the two adjacent FL^{2-} anions to stack in a head-to-tail fashion (Scheme 1A) in order to produce minimum steric hindrance. However, only one TTP cation in [TTP][FL] allows the two FL^{-} anions to stack primarily in a random fashion. Therefore, this resembles the spectral behaviour of the monomeric species and partly stacks into head-to-tail manner (J-type of aggregates) (Scheme 1B).

Examination of data from photostability studies of $[TTP]_2[FL]$ nanoparticles indicated extremely high photostability upon prolonged (2500 s) irradiation under maximum exposure (Figure S4). The photostability of $[TTP]_2[FL]$ in ethanolic solution were found to increase under similar conditions (data not shown). Such an effect was also observed in previous studies and was attributed to irradiation induced J-aggregation.[28] We note that photostability of fluorescent nanomaterials is an extremely important factor for determining sensor applicability in adverse conditions. Thus, the observed enhanced photostability in solutions and extremely high (100 %) photostability of the nanodroplets of these materials are considered an additional advantage of the materials.

Fluorescence anisotropy (FA) studies of the [TTP]2[FL] nanodroplets (Figure 3) also suggest a change in molecular aggregation with variation in values of pH, exhibiting negative and lower FA values in water and at pH 7.4 where J-aggregation is maximum. FA was found to increase with increasing acidity of the buffer, suggesting alteration in molecular stacking and formation of different types of aggregates. J-aggregates have often been reported to demonstrate lower, as well as negative FA upon excitation at a wavelength blue to the J-band. This is attributed to faster exciton relaxation and energy migration as compared to randomly oriented or H-type aggregates.[18,29] FA studies provide a molecular level picture of the nanodroplets, and provides a better understanding of the intermolecular aggregation behaviour under various pH conditions.

Morphological Changes in TTP Nanomaterials with Changes in pH

The pH dependent colorimetric response was also accompanied by a change in particle size, as illustrated in the transmission electron microscopic images (Figure 3) of the $[TTP]_2[FL]$ nanodroplets. These nanodroplets demonstrated a size of 28±8 nm at pH 7.4, gradually increasing in size with lowering of pH, attaining a size of 1.6 ± 0.2 μm μm at pH 4, followed by appearance of two distinctly different sizes at pH 2.2 viz. 797 ± 171 nm, 167 ± 46 nm (Figure 4). This observation was also complemented by data obtained from dynamic light scattering (DLS) (Table 1). Examination of data from DLS studies indicated similar

expansion of the nanodroplets with decreasing pH up to pH 4, followed by a sudden drop in size at pH 2.2 accompanied with some micron sized particles. It was noted during these studies that the nanodroplet dispersions were extremely stable for hours with insignificant particle growth or change in surface charge over time.

Examination of TEM micrographs indicates relatively less dense mesodroplets in the acidic environments which is recognized as an effect of expansion in these media. One possible explanation for the observed nanoparticle swelling is attributed to an alteration in molecular stacking within the nanodroplets under various pH conditions due to the formation of various protolytic states of FL. It has been reported in the literature that both covalent and non-covalent interactions such as π-π interaction play a significant role in molecular organization at the nanoscale level.[30] Fluorescein is known to exist in four protolytic forms with dissociation constants (pKa values) of 2.08, 4.31 and 6.43 corresponding to respective transitions from cationic to neutral, neutral to monoanionic, and monoanionic to dianionic.[22] The neutral to monoanionic and monoanionic to dianionic protolytic constants were determined for $[TTP]_2[FL]$ using UV-visible spectrophotometry and were found to be 4.52 and 6.37, respectively. These values are very close to the reported values for disodium fluorescein. Thus, the smallest particle size was obtained when fluorescein was in its dianionic form (water and pH 7.4) within the $[TTP]_2[FL]$ nanodroplets, which corresponds to an ordered head-to-tail type of stacking as suggested by examination of the absorption and fluorescence steady state spectra, as well as time domain measurements. Monoprotonation of fluorescein at pH 5.4 leading to its monoanionic form disturbs this ordered arrangement, as suggested by shifts in the absorption and fluorescence properties resulting in swelling. A further disordered arrangement ensues when the neutral form of fluorescein is formed at pH 4 which in combination with the hydrophobic phosphonium cations, resulting in an additional increase in particle size. However, the formation of cationic fluorescein at pH 2.2 should lead to repulsion with the phosphonium cations, possibly causing complete deformation of the pre-existing particles and formation of smaller particles of a different size distribution. Both fluorescein and phosphonium cations under such conditions are obviously considered to be associated with other counterions present in the buffer. The changes in ionic states of fluorescein with variation of pH values, affect the number of TTP ions associated with each FL, as well as the ionic and other non-covalent interactions within the particles. This change in interactions leads to different molecular orientations and stackings within the nanomaterial which contributes to the color changes of the dispersion.

Examination of zeta potential measurements indicates a systematic change in surface charge with varying pH. The variation in molecular orientation at various pH values possibly contributes to the variable surface charge. In water and at pH 7.4, the surface charge was highly positive (~ +40mV) (Table S1) which is also consistent with the observed high stability of these particles. The surface charge becomes less positive with lower pH values and then becomes negative. The surface charge is nearly zero at pH 4 and attains a high positive value at pH 2. The change in zeta potential (Table S1) of the particles at different pH values may also indicate altered orientations and the presence of variable numbers of TTP ions associated with different ionic forms of FL. A highly positive zeta potential at pH 2.2 is attributed to the presence of both fluorescein and phosphonium cations under such

conditions. Similarly, a very small value of zeta potential at pH 4 can be attributed to the presence of neutral fluorescein at this pH. In addition, the presence of monoanionic FL at pH 5.5, where one TTP cation is associated with one FL, yields a net negative surface charge. However, two TTP cations associated with the dianionic FL present at a physiological pH results in a net positive surface charge. Thus it is the molecular orientation and the presence of various ionic forms of FL under various pH conditions which determine the net charge on the nanoparticles.

In addition to these two ILs, four other posphonium based disubstituted and monosubstituted ILs were synthesized through ion-exchange with the tetrabutyl phosphonium, benzyltriphenylphosphonium, 4-nitrobenzyltriphenyl phosphonium, and tetraphenyl phosphonium counterions and their pH dependent characteristics were studied. A pH dependent color change was not observed for any of these ILs, including the parent sodium salt. Thus, the observed pH dependent properties appear to be a unique characteristic of the nanoparticles based on $[TTP]_2[FL]$.

Conclusions

In summary, two novel fluorescent pH dependent IL based nanomaterials have been successfully synthesized and characterized. The pH dependent colorimetric response of $[TTP]_2[FL]$ nanodroplets suggests possible applications of these materials for determination of acidosis *in vitro* or *in vivo* as biosensor for cancer and bacterial infections. The change in size of the nanodroplets with decrease of pH as suggested from the TEM and DLS studies may also be exploited for pH dependent molecular recognition as well as pH dependent drug delivery vehicles.[31] The considerably large zeta potentials of these nanoparticles also suggest their stability in solution. In addition alterations in fluorescence properties with values of pH may also be utilized in fluorescence imaging to detect various pathological conditions.

Experimental

Materials

Trihexyltetradecylphosphonium chloride, disodium fluorescein, tetrabutylphosphonium chloride, benzyltriphenylphosphonium chloride, 4-nitrobenzyltriphenylphosphonium chloride and tetraphenylphosphonium chloride were purchased from Sigma Aldrich and were used as received. Citric acid (Sigma Aldrich), sodium phosphate dibasic heptahydrate (Fisher Scientific), and sodium phosphate monobasic monohydrate (Fisher Scientific) were used for the preparation of universal buffer (pH 2.2 - pH 5.5)[24] and phosphate buffer (pH 7.4). Triply deionized water (18.2 MΩ cm), obtained from an Elga model PURELAB ultra water-filtration system, was used for the preparation of all the solutions.

Synthesis and Characterization of the ILs

$[TTP]_2[FL]$ was synthesized by exchanging the two sodium ions of disodium fluorescein (Na_2FL) with trihexyltetradecylphosphonium (TTP) cations of trihexyltetradecylphosphonium chloride (TTPCl) by carrying out the exchange with 2:1 ratio of TTPCl and Na_2FL (Scheme 2a). The second IL was obtained by ion-exchange reaction of

monosodium fluorescein with the same phosphonium cation (1:1) to yield [TTP][FL] (Scheme 2b). The monosodium fluorescein was synthesized by monoprotonation of Na_2FL by stirring it in a buffer of pH 5.[22] The detailed syntheses of the ionic liquids are providesd in the supporting information. Characterization of the synthesized ILs were accomplished using FTIR, ^1H NMR, and mass spectrometry (supporting information). The formation of the 1:1 and 2:1 stoichiometries were confirmed by integrated ^1H NMR. Other phosphonium salts of fluorescein were also synthesized using similar approaches.

Nanomaterials Synthesis

Nanomaterials were synthesized from the ILs using a modified simple, additive-free reprecipitation method similar to that used for organic nanoparticles.[32] In a typical preparation, 250 μL of a 1 mM solution of GUMBOS precursor dissolved in ethanol was rapidly injected into 5 mL of triply-deionized water in an ultrasonic bath, followed by additional sonication for 2 min. All solvents used in this study were filtered prior to nanoparticle preparation using 0.2 μm nylon membrane filters. The particles were allowed a 15 min of equilibriation time after preparation and then characterized using different techniques.

Characterization of size and morphology of the nanomaterials

The average particle size and size distribution of the prepared nanomaterials were obtained by use of transmission electron microscopy (TEM). TEM micrographs were obtained using an LVEM5 transmission electron microscope (Delong America, Montreal, Canada). The nanoGUMBOS dispersion (1 μL) were drop casted onto a carbon coated copper grid and allowed to dry in air at room temperature before TEM imaging. The numerical average of the particle sizes were determined by counting more than 200 particles captured on various mages for each sample using the software associated with the instrument. DLS studies for size determination of nanomaterials were performed using with a Malvern Zetasizer, UK. Zeta potential of the nanomaterials were also determined used the same set up.

Absorption and fluorescence studies

Absorbance measurements were performed using a Shimadzu UV-3101PC, an UV-Vis-near-IR scanning spectrometer (Shimadzu, Columbia, MD). Fluorescence studies were performed using a Spex Fluorolog-3 spectrofluorimeter (model FL3-22TAU3); Jobin Yvon, Edison, NJ). A 0.4 cm path length quartz cuvette (Starna Cells) was used for acquiring the fluorescence and absorbance against an identical cell filled with water as the blank. Fluorescence studies were performed adopting a synchronous scan protocol with right angle geometry. Fluorescence spectra were corrected for inner filter effects using a standard formula.[33] Fluorescence anisotropy(r) is a measure of the average angular displacement of the fluorophore between the absorption and subsequent emission of the photon and is given by the formula

$$r=(Ivv - GIvh)/(Ivv+2GIvh) \quad (1)$$

where G is the grating factor that has been included to correct for the wavelength response for polarization of the emission optics and the detector. The parameters, Ivv and Ivh, are the

fluorescence emission intensity measured parallel and perpendicular to the vertically polarized excitation, respectively. The parameters, Ihh and Ihv, are the fluorescence emission intensity measured parallel and perpendicular to the horizontally polarized excitation.[33] Fluorescence lifetime measurements were performed at Horiba Jobin Yvon, NJ using time domain mode. A picoseconds pulsed excitation source of 450 nm was used and emission was collected at 545 nm for $[TTP]_2[FL]$ and 515 nm for [TTP][FL] with a TBX detector. The time correlated single photon counting (TSCPC) mode was used for data acquisition with a resolution of 7 ps/channel.

Supplementary Material

Refer to Web version on PubMed Central for supplementary material.

Acknowledgments

Isiah M. Warner acknowledges financial support from the National Science Foundation (grant no. grant no. CHE-1307611) and National Institute of Health (grant no. 1R01GM079670).

Bibliographic References and Notes

1. Song YJ, Wei WL, Qu XG. Advanced Materials. 2011; 23(37):4215–4236. [PubMed: 21800383]
2. Gao LZ, Zhuang J, Nie L, Zhang JB, Zhang Y, Gu N, Wang TH, Feng J, Yang DL, Perrett S, Yan X. Nature Nanotechnology. 2007; 2(9):577–583.
3. Asati A, Santra S, Kaittanis C, Nath S, Perez JM. Angewandte Chemie-International Edition. 2009; 48(13):2308–2312.
4. Liu JW, Lu Y. Angewandte Chemie-International Edition. 2006; 45(1):90–94.
5. Gillies RJ, Raghunand N, Garcia-Martin ML, Gatenby RA. IEEE Engineering in Medicine and Biology Magazine. 2004; 23(5):57. [PubMed: 15565800]
6. Pichavant L, Bourget C, Durrieu MC, Heroguez V. Macromolecules. 2011; 44(20):7879–7887.
7. Soppimath KS, Liu LH, Seow WY, Liu SQ, Powell R, Chan P, Yang YY. Advanced Functional Materials. 2007; 17(3):355–362.
8. Saha S, Chakraborty K, Krishnan Y. Chemical Communications. 2012; 48(19):2513–2515. [PubMed: 22278189]
9. Thanh NTK, Rosenzweig Z. Analytical Chemistry. 2002; 74(7):1624–1628. [PubMed: 12033254]
10. Liu LX, Li W, Liu K, Yan JT, Hu GX, Zhang AF. Macromolecules. 2011; 44(21):8614–8621.
11. Baker GA, Baker SN, Pandey S, Bright FV. Analyst. 2005; 130(6):800–808. [PubMed: 15912225]
12. Yung KY, Schadock-Hewitt AJ, Hunter NP, Bright FV, Baker GA. Chemical Communications. 2011; 47(16):4775–4777. [PubMed: 21399813]
13. Zhang QH, Zhang SG, Liu SM, Ma XY, Lu LJ, Deng YQ. Analyst. 2011; 136(7):1302–1304. [PubMed: 21305085]
14. Benito-Lopez F, Coyle S, Byrne R, O'Toole C, Barry C, Diamond D. International Conference on Body Sensors Network. 2010:291–296.
15. Lee Y-EK, Kopelman R, Smith R. Annu Rev Anal Chem (Palo Alto Calif). 2009; 2:57–76. [PubMed: 20098636]
16. Li M, De Rooy SL, Bwambok DK, El-Zahab B, DiTusa JF, Warner IM. Chemical Communications. 2009; 45:6922–6924. [PubMed: 19904348]
17. de Rooy SL, El-Zahab B, Li M, Das S, Broering E, Chandler L, Warner IM. Chemical Communications. 2011; 47(31):8916–8918. [PubMed: 21674099]
18. Das S, Bwambok D, El-Zahab B, Monk J, de Rooy SL, Challa S, Li M, Hung FR, Baker GA, Warner IM. Langmuir. 2010; 26(15):12867–12876. [PubMed: 20583774]
19. Sun H, Gu H, Scharff-Poulsen AM, Almdal K. Chem. Mater. 2006; 18(15):3381.

20. Ghaemy M, Naseri M. Carbohydrate Polymers. 2012; 90:1265–1272. [PubMed: 22939340]
21. Griset AP, Walpole J, Liu R, Gaffey A, Colson YL, Grinstaff MW. J. Am. Chem. Soc. 2009; 131:2469–2471. [PubMed: 19182897]
22. Sjoback R, Nygren J, Kubista M. Spectrochimica Acta Part a-Molecular and Biomolecular Spectroscopy. 1995; 51(6):L7–L21.
23. Del Popolo MG, Voth GA. Journal of Physical Chemistry B. 2004; 108(5):1744–1752.
24. McIlvaine TC. Journal of Biological Chemistry. 1921; 49(1):183–186.
25. Berlepsch HV, Bottcher C. Langmuir. 2013; 29:4948–4958. [PubMed: 23527663]
26. De S, Das S, Girigoswami A. Spectrochimica Acta Part a-Molecular and Biomolecular Spectroscopy. 2005; 61(8):1821–1833.
27. Lin HZ, Camacho R, Tian YX, Kaiser TE, Wurthner F, Scheblykin IG. Nano Letters. 2010; 10(2): 620–626. [PubMed: 20043661]
28. Lu C, Das S, Magut PKS, Li M, El-Zahab B, Warner IM. Langmuir. 2012; 28:14415–14423. [PubMed: 22957476]
29. Scheblykin IG, Drobizhev MA, Varanavsky OP, Auweraer MV-D, Vitukhnovsky AG. Chem. Phys. Lett. 1996; 261:181–190.
30. Jia H, Bai XT, Shi LJ, Lu F, Zheng LQ. Nanoscale. 2012; 4(10):3162–3167. [PubMed: 22535258]
31. Dalmau M, Lim SR, Wang SW. Nano Letters. 2009; 9(1):160–166. [PubMed: 19113890]
32. Kasai H, Kamatani H, Okada S, Oikawa H, Mastuda H, Nakanishi H. Jpn. J. Appl. Phys. 1996; 35:L221–L223.
33. Lackowicz, JR. Principles of Fluorescence Spectroscopy. Plenum; New York: 1983.

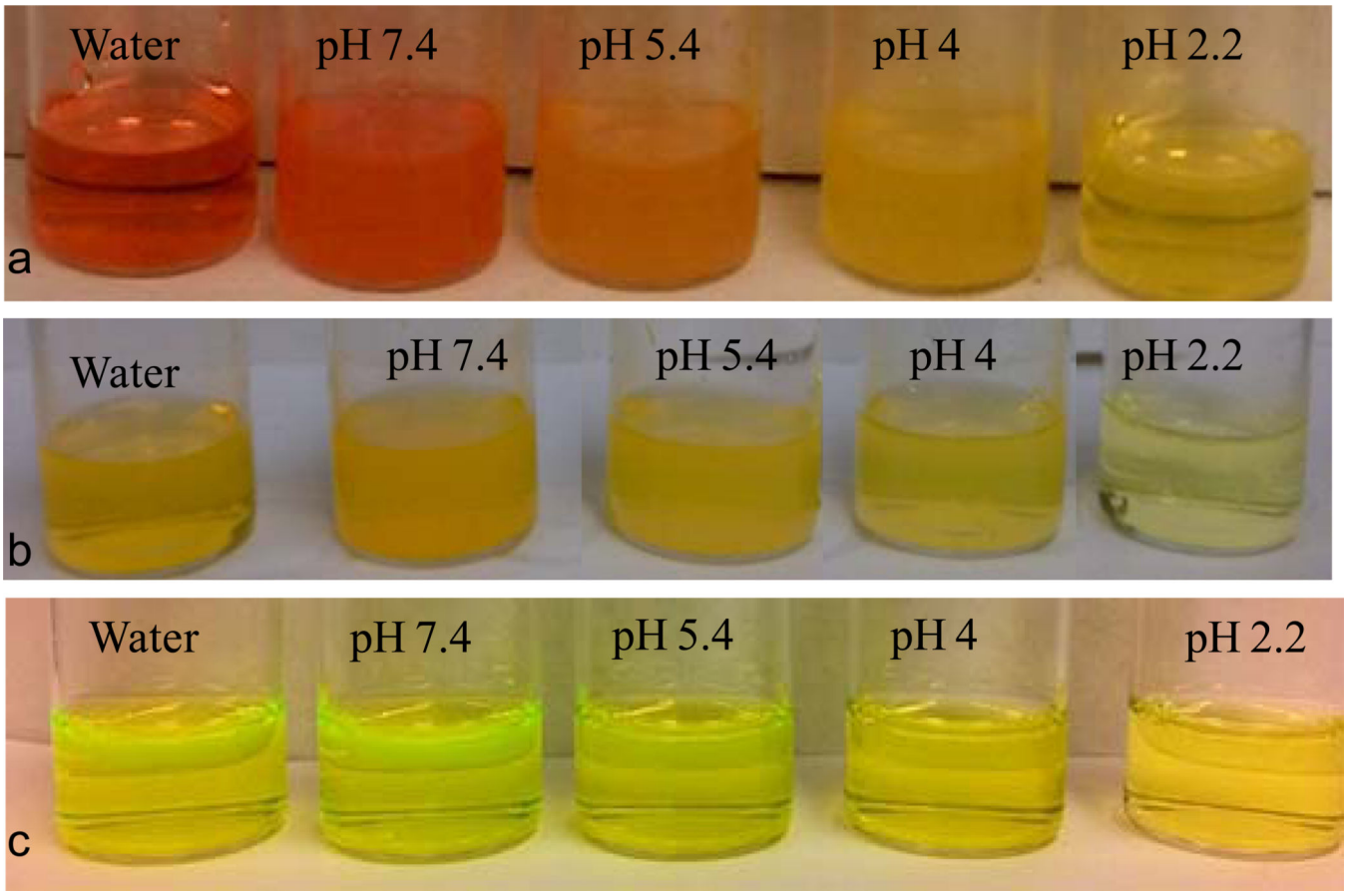

Figure 1.

pH dependent color change of (a) $[TTP]_2[FL]$ nanodroplets, (b) [TTP][FL] nanoparticles and (c) Na_2FL in water (inherent pH 8.3) and buffers of different pH.

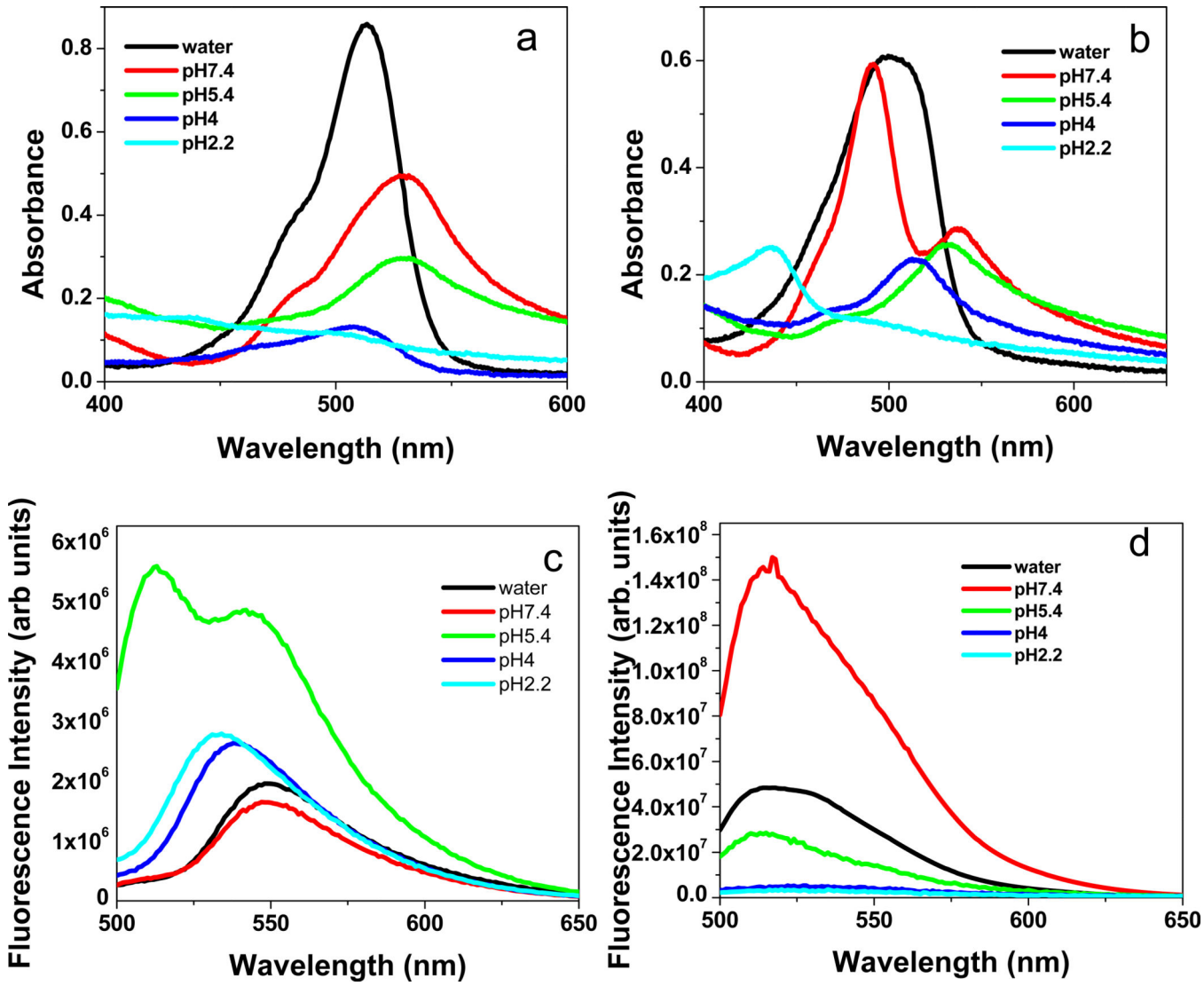

Figure 2.

(a) and (c) absorption and fluorescence spectra of $[TTP]_2[FL]$ and (b) and (d) of [TTP][FL], respectively.

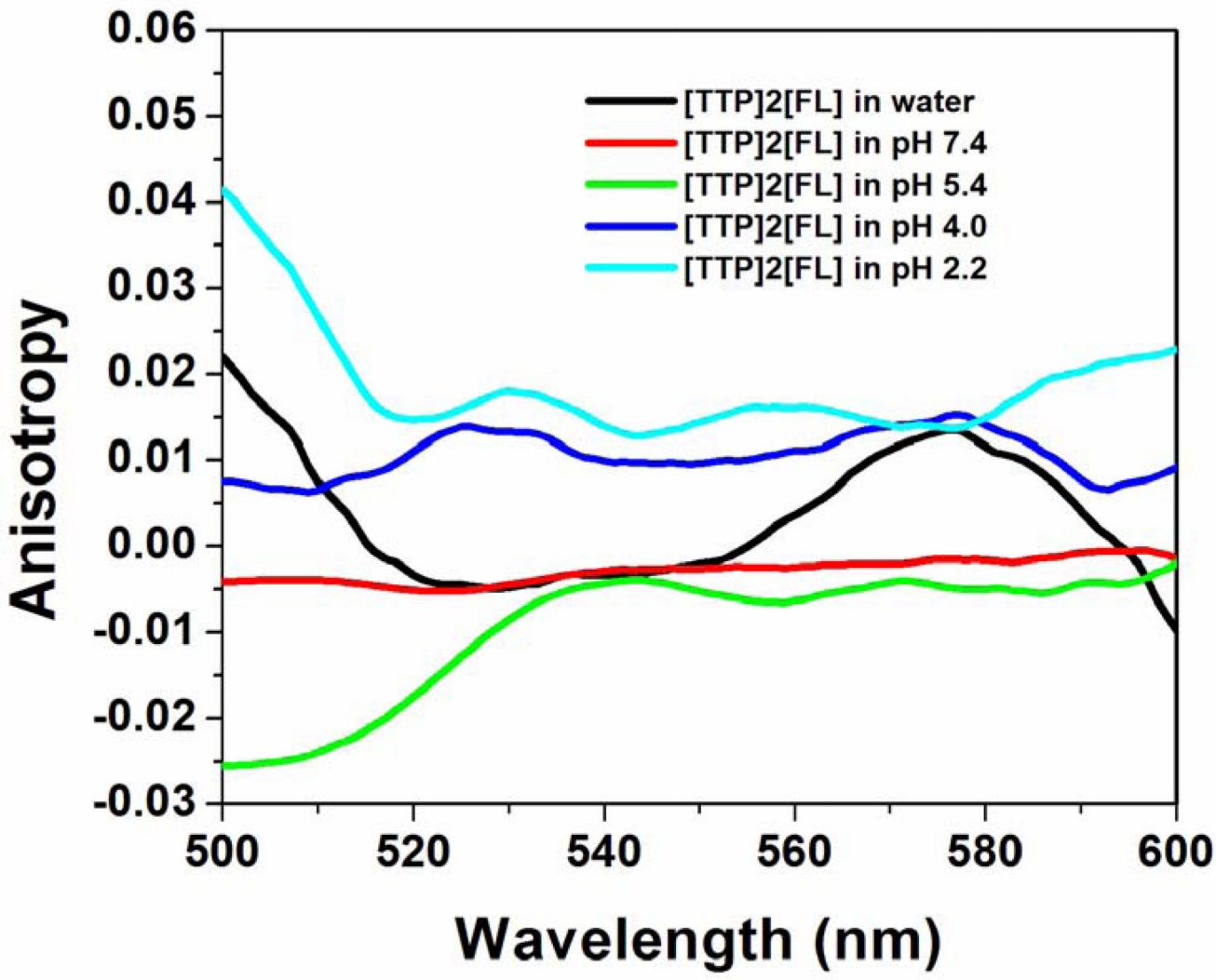

Figure 3.
Fluorescence emission anisotropy of [TTP]2[FL] nanodroplets in buffer of varying pHs.

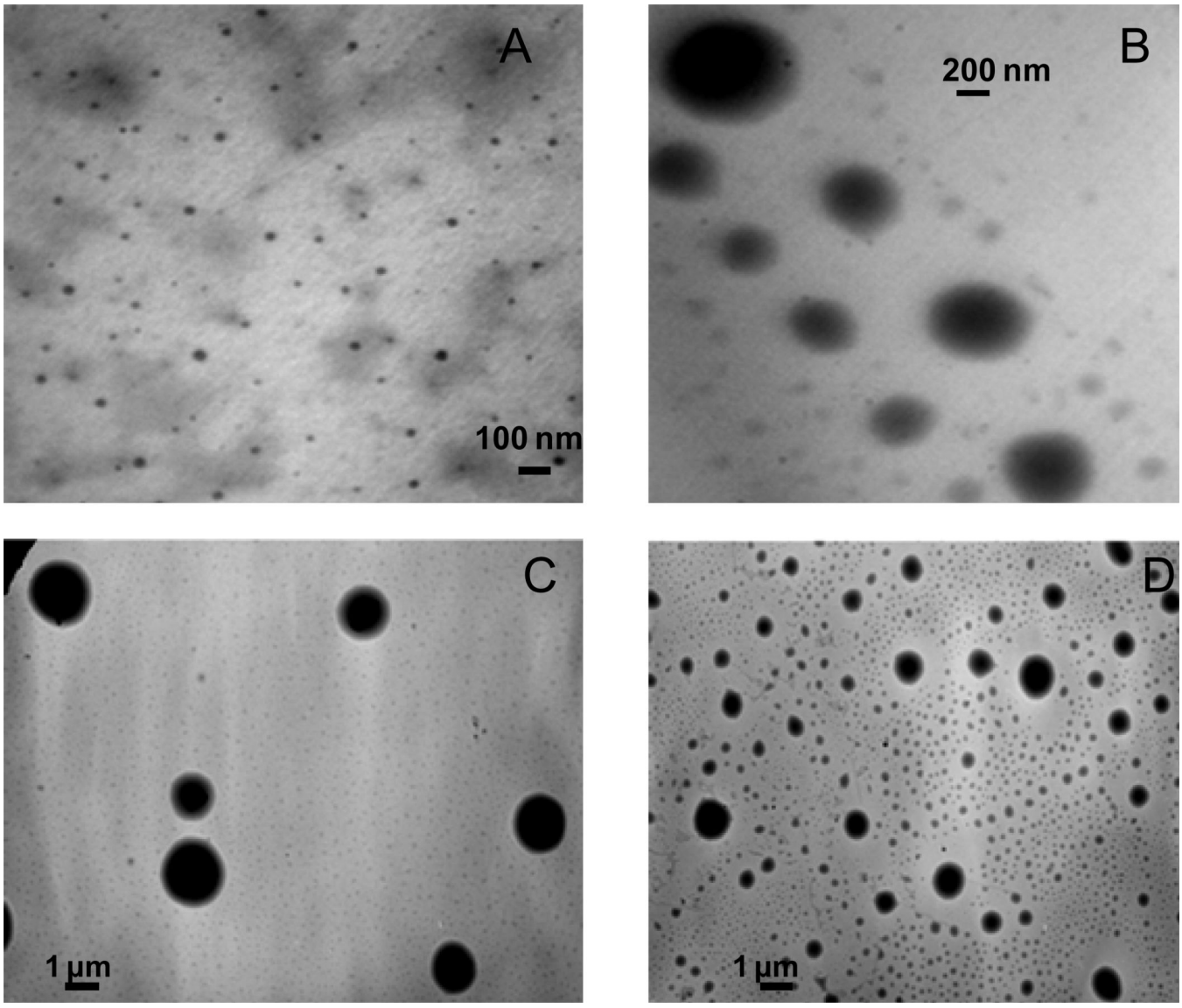

Figure 4.

TEM micrographs of $[TTP]_2[FL]$ nanoparticles in (A) water (pH 8.3) (28 ± 8 nm nm) and buffers of (B) pH 5.4 (453 ± 197 nm) , (C) pH 4.0 (1.6 ± 0.2 μm), (D) pH 2.2 (797 ± 171 nm, 167 ± 46 nm).

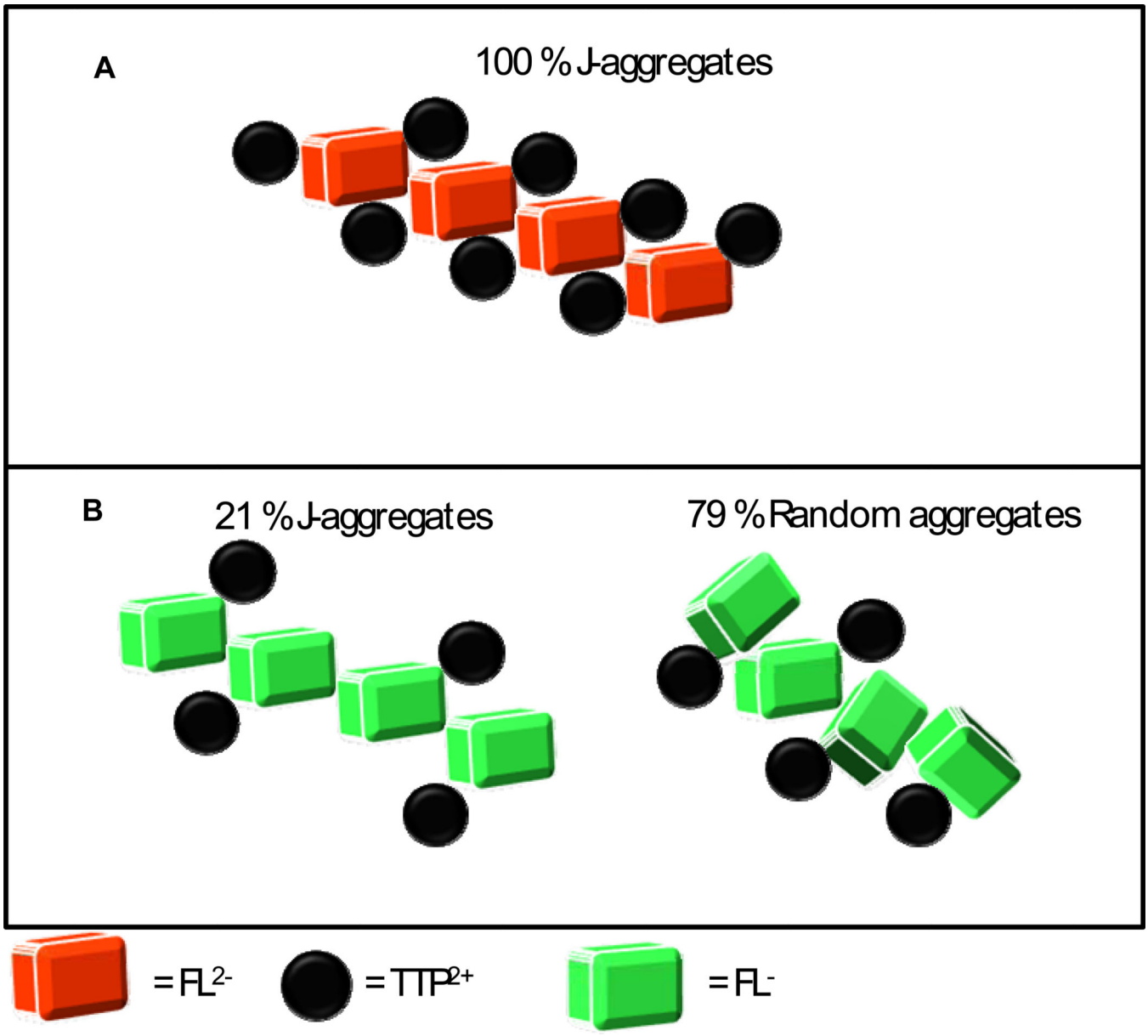

Scheme 1.
Schematic representation of the type of aggregation in (A) $[TTP]_2[FL]$ and (B) [TTP][FL].

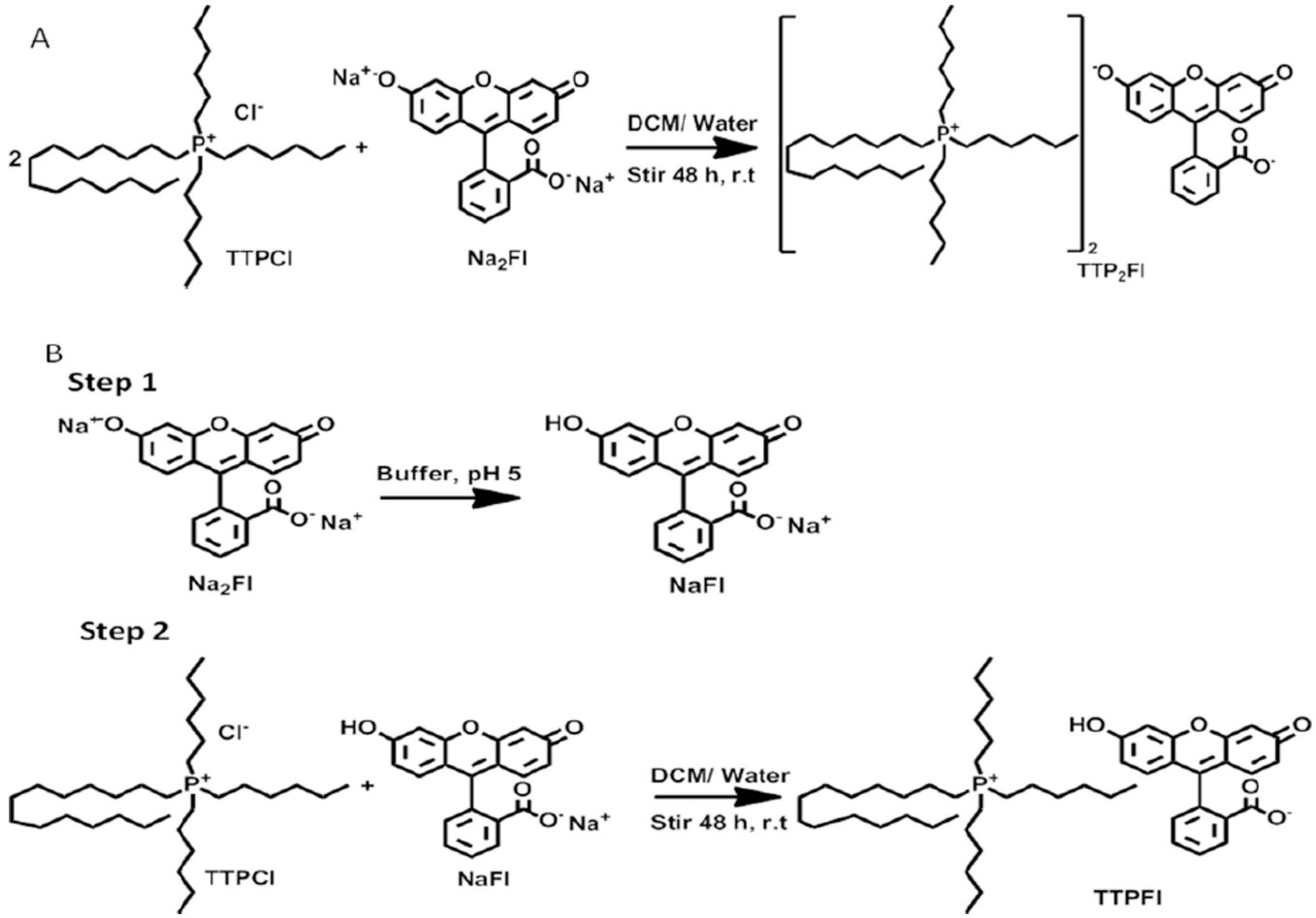

Scheme 2.
Reaction mechanism for synthesis of (A) [TTP]2[FL] and (B) [TTP][FL] ionic liquids

Table 1

Size of $[TTP]_2[FL]$ and [TTP][FL] nanodroplets at various pH values obtained from DLS.

System	Peak 1 (nm)	Peak1 ar. Int. (%)	Peak 2 (nm)	Peak 2 ar. Int. (%)	Z-average (nm)	Polydispersity index (PDI)
$[TTP]_2[FL]$ in water	85.8	100	-	-	77.1	0.144
$[TTP]_2[FL]$ in pH 7.4	173.9	100	-	-	188.3	0.18
$[TTP]_2[FL]$ in pH 5.4	763	100	-	-	874	1
$[TTP]_2[FL]$ in pH 4.0	1592	100	-	-	1592	1
$[TTP]_2[FL]$ in pH 2.2	124.5	98.8	2490	1.2	114.7	0.141
[TTP][FL] in water	100.7	100	-	-	96.62	0.088
[TTP][FL] in pH 7.4	534.7	100	-	-	538.1	0.039
[TTP][FL] in pH 5.4	402.4	100	-	-	521.1	0.057
[TTP][FL] in pH 4.0	795.9	100	-	-	717.4	0.17
[TTP][FL] in pH 2.2	124.1	100	-	-	115.1	0.108